[4] Hughes, T. P., and K. M. Young, *Nature*, vol 196, 1962, p 332.
[5] Evtuhov, V., and J. K. Neeland, *Appl. Optics*, vol 2, 1963, p 319.
[6] Fox, A. G., and T. Li, *Bell Sys. Tech. J.*, vol 40, 1961, p 453.
[7] Boyd, G. D., and J. P. Gordon, *Bell Sys. Tech. J.*, vol 40, 1961, p 489.
[8] Boyd, G. D., and H. Kogelnik, *Bell Sys. Tech. J.*, vol 41, 1962, p 1347.
[9] Fox, A. G., and T. Li, Modes in a maser interferometer with curved and tilted mirrors, PROC. IRE, vol 51, 1963, pp 80–89.
[10] Boyd, G. D., *Quantum Electronics*, vol III, P. Grivet and N. Bloembergen, Eds. New York: Columbia University Press, 1964, p 1173.
[11] Evtuhov, V., and J. K. Neeland, *ibid.*, p 1405.
[12] Stickley, C. M., *Appl. Optics*, vol 3, 1964, p 967.
[13] Maiman, T. H., R. H. Hoskins, I. J. D'Haenens, C. K. Asawa, and V. Evtuhov, *Phys. Rev.*, vol 123, 1961, p 1151.
[14] Ciftan, M., A. Krutchkoff, and S. Koozekanani, On the resonant frequency modes of ruby optical masers, *Proc. IRE*, (*Correspondence*) vol 50, 1962, pp 84–85.
[15] Wagner, W. G., and G. Birnbaum, *J. Appl. Phys.*, vol 32, 1961, p 1185.
[16] Haken, H., and H. Sauermann, *Z. Physik*, vol 173, 1963, p 261.
[17] Tang, C. L., H. Statz, and G. deMars, *J. Appl. Phys.*, vol 34, 1963, p 2289.
[18] Bennett, W. R., Jr., *Phys. Rev.*, vol 126, 1962, p 580.
[19] Tang, C. L., H. Statz, and G. deMars, *Appl. Phys. Lett.*, vol 2, 1963, p 222.
[20] Tang, C. L., H. Statz, G. A. deMars, and D. T. Wilson, *Phys. Rev.*, vol 136, 1964, p A1.
[21] Evtuhov, V., *Appl. Phys. Lett.*, vol 6, Apr 1965.
[22] Statz, H., and C. L. Tang, *J. Appl. Phys.*, vol 35, 1964, p 1377.
[23] Rigrod, W. W., *Appl. Phys. Lett.*, vol 2, 1963, p 51.
[24] Evtuhov, V., and J. K. Neeland, Mode control in a ruby laser, *21st Annual Conf. on Electron Device Research*, Jun 1963 (unpublished).
[25] Siegman, A. E., R. J. Morris, and R. Wilson, Ruby laser mode control with small mirrors, *21st Annual Conf. on Electron Device Research, Jun 1963 (unpublished)*; Siegman, A. E., *1964 Meeting of the American Optical Society*, Abstract TB14.
[26] Suematsu, Y., and K. Iga, Experiment on quasi-fundamental mode oscillation of ruby laser, *Proc. IEEE*, (*Correspondence*) vol 52, 1964, pp 87–88.
[27] Forrester, A. T., *Advances in Quantum Electronics*, vol II, J. R. Singer, Ed. New York: Columbia University Press, 1961, p 233.
[28] McMurtry, B. J., and A. E. Siegman, *Appl. Optics*, vol 1, 1962, p 51.
[29] Silver, M., R. S. Witte, and C. M. York, *Bull. Am. Phys. Soc.*, vol 8, 1963, p 380. ——*Appl. Optics*, vol 3, 1964, p 539.
[30] Adamson, M. C., T. P. Hughes, and K. M. Young, *Quantum Electronics*, vol III. New York: Columbia University Press, 1964, p 1459.
[31] Stickley, C. M., *Appl. Optics*, vol 2, 1963, p 855.
[32] Tonks, L., *J. Appl. Phys.*, vol 33, 1962, p 1980.

Characteristics of Mode-Coupled Lasers

M. H. CROWELL, MEMBER, IEEE

Abstract—**The effects of mode-coupling in a gas laser resulting from a time-varying loss within the optical cavity or from the nonlinear characteristics of the inverted population are investigated both theoretically and experimentally. The dominant effect resulting from this mode-coupling is that the laser operates as a pulse regenerative oscillator which produces a periodic train of subnanosecond width pulses. The exact repetition frequency is determined by the frequency of the time-varying loss, which must always be set close to a multiple of $c/2L$, i.e., the axial mode spacing, to produce sufficient coupling. To produce pulsing without a time-varying loss, it is necessary that the Q or loss of the cavity be judiciously adjusted. In this case the repetition frequency is very close to the axial mode spacing. A preliminary experimental investigation has verified the salient features of the analysis. The measured widths of the pulses from a 6328 Å He-Ne laser and from a 4880 Å Argon-Ion laser were 0.5 and 0.25 ns, respectively.**

I. INTRODUCTION

THE OPTICAL MODES in a laser may be coupled by inserting a time-varying loss into the cavity or by the nonlinear gain characteristics of the inverted population.[1] Mode-coupling from either of these two mechanisms causes the laser to operate as a pulse regenerative oscillator in a manner that is directly analogous to the microwave pulse regenerative oscillator described by Cutler [1]. Cutler determined the characteristics of the microwave oscillator by describing it in terms of a closed-loop system and by analyzing the effect of a pulse traversing the closed-loop.

The results obtained here, as well as those reported in DiDomenico [2] and Yariv [3], were obtained by expanding the electric and magnetic fields in the cavity in terms of normal modes. In general, the coupled differential equations that one obtains when the fields in the cavity are expressed in the normal mode representation predict time-varying mode amplitudes. The transient solutions resulting from these time-varying mode amplitudes are quite complex and will not be discussed in this paper.

Approximate steady-state solutions for the laser, when it operates as a pulse regenerative oscillator, can be determined by examining the conditions that predict time-invariant mode amplitudes. The degree of approximation is such that any solution obtained in this manner should be evaluated in terms of experimental observations before it is considered meaningful.

From a historical point of view, Hargrove et al. [4], were the first to operate a laser (He–Ne 6328 Å) as a pulse regenerative oscillator. Guided by his experimental results, DiDomenico, in collaboration with E. I. Gordon, was able to predict some of Hargrove's observations, particularly the pulse shape, by solving a restricted set of normal mode equations. DiDomenico assumed in his analysis that the frequency of the time-varying loss was

Manuscript received February 1, 1965.
The author is with Bell Telephone Labs., Inc., Murray Hill, N. J.
[1] The pulsating output from a 6328 Å He–Ne laser with naturally coupled modes, was described at the 1964 PGED Meeting, Washington, D. C.

exactly equal to some multiple of the fundamental cavity resonance or axial mode spacing, i.e., $c/2L$, and also that the gain of the medium, expressed in terms of a volume conductivity, was self-adjusting to provide a stable solution.

Experimentally, the frequency of the time-varying loss need not be exactly equal to a multiple of the fundamental cavity resonance. The analysis here is more general than the one presented by DiDomenico since the frequency of the time-varying loss is restricted only to be close to the fundamental cavity resonance. Furthermore, the gain of the medium is represented as a volume polarization which depends upon the discharge excitation, optical fields, and position. The technique of expressing the gain of the medium as a volume polarization is discussed by Lamb [5] in detail.

It has been observed that the mode-coupling resulting from the nonlinear volume polarization in an He–Ne 6328 Å laser will cause the laser to operate as a pulse regenerative oscillator. It is possible to provide some theoretical justification for this self-pulsing condition from Lamb's analysis. However, Lamb restricted the validity of his analysis by assuming that the mirrors of the cavity were lossless. Thus, it was necessary to introduce a loss into the cavity by assuming that a fictitious optical conductivity permeated the entire cavity. Consequently, the resulting modal solutions represented perfect standing waves. The main consequence of this restriction was that the derived frequency pulling and the mode-coupling resulting from the inverted populated were more grossly approximated than necessary. Although Lamb described how the modes might be coupled by the nonlinear relationship between the polarization vector and the electric field, he described the effect of this mode-coupling only in terms of the RF-beat frequencies generated by a square-law photodetector rather than the envelope of the optical output.

Section II will be devoted to a detailed treatment of mode-coupling produced by internal modulation. Particular attention will be given to displaying the results in terms of experimentally measurable parameters, e.g., average laser power, peak pulse power, pulse position and width, etc., as a function of the difference between the modulation frequency and the axial mode spacing as well as the position of the modulator in the cavity. This section will be followed by a description of the experimental results and a comparison with theory. A final section will be devoted to a description of self-pulsing.

II. Resonant Intracavity Modulation

The technique for obtaining intracavity modulation is shown in Fig. 1. The laser consists of a gas discharge with two spherical mirrors external to the discharge. At a distance Z_0 from one mirror an acoustic diffraction grating is inserted into the cavity. A quartz transducer is used to launch a longitudinal acoustic wave into the fused quartz. The light passes through the fused quartz at Brewster's angle. The standing acoustic wave in the

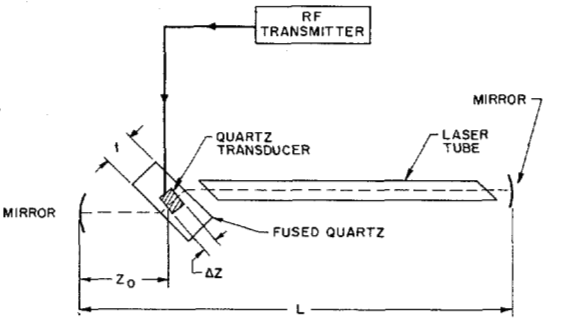

Fig. 1. Intracavity modulator.

fused quartz creates an acoustic diffraction grating. It has been shown that the volume diffraction grating attenuates the zero order beam by scattering energy into higher order beams [6], [7]. Furthermore, since the standing wave disappears twice during each period of the applied RF, the attenuation of the lowest order beam varies at twice the acoustic frequency.

The source of this attenuation may be represented as a fictitious optical conductivity that varies in time as

$$\sigma(t) = \begin{cases} \sigma_1[1 - \cos\omega_0(t - t_1)] & \text{for } |Z - Z_0| \leq \dfrac{\Delta Z}{2} \\ 0 & \text{for } |Z - Z_0| > \dfrac{\Delta Z}{2} \end{cases} \tag{1}$$

where the thickness of the acoustic diffraction grating in the fused quartz, i.e., the modulator, is ΔZ, and ω_0 is equal to twice the applied RF radian frequency.

This analysis will be restricted to adjacent mode-coupling. Thus, ω_0 will be approximately equal to the axial mode spacing, i.e., $\omega_0 \approx \pi c/L$.

The magnitude of the fictitious conductivity is proportional to the ratio optical power scattered by the grating to the optical power incident on the grating. This may be expressed as

$$\sigma_1 = \frac{\sqrt{\epsilon_1}}{377\Delta Z}\left[\frac{\text{optical power scattered}}{\text{optical power incident}}\right] \text{mhos}/m^3 \tag{2}$$

where $\sqrt{\epsilon_1}$ is the index of refraction for the fused quartz.

It will be convenient to express the magnitude of this conductivity in terms of a dielectric Q for a particular optical frequency ω_n as

$$Q_\sigma^{-1} = \frac{\sigma_1}{\omega_n\langle\epsilon\rangle}\left(\frac{\Delta Z}{L}\right) \tag{3}$$

where $\Delta Z/L$ is a filling factor term associated with the fact that the modulator occupies only a fraction of the length, L, of the cavity and $\langle\epsilon\rangle$ is an effective permittivity for the electric field.[2]

[2] With the modulator geometry shown in Fig. 1, the acoustic diffraction grating may be created in only a portion of the fused quartz. Thus, the filling factor term for the conductivity may be different from the filling factor term for the dielectric constant.

With these assumptions and definitions, Maxwell's equations may be written for the fields in the cavity as

$$\nabla \times \mathbf{H} = \sigma \mathbf{E} + \epsilon \frac{\partial \mathbf{E}}{\partial t} + \frac{\partial \mathbf{P}}{\partial t} \tag{4}$$

and

$$\nabla \times \mathbf{E} = -\mu_0 \frac{\partial \mathbf{H}}{\partial t} \tag{5}$$

where $\mathbf{P}$ is the polarization vector that describes the laser medium and σ is defined in (1).

A. Mode Equations

The purpose of this subsection is to obtain a second-order partial differential equation that represents the exact relationship between the normal modes and to illustrate the fundamental differences between this analysis and those described in the literature.

Following the technique described by Slater [8] and used by Gordon and Rigden [9] the fields may be expressed in terms of normal modes as[3]

$$\mathbf{E}(\mathrm{r}, t) = \sum_a e_a(t)\mathbf{E}_a(\mathrm{r}) \tag{6}$$

and

$$\mathbf{H}(\mathrm{r}, t) = \sum_a h_a(t)\mathbf{H}_a(\mathrm{r}) \tag{7}$$

where e_a and h_a are the mode amplitudes associated with the set of orthonormal modes $\mathbf{E}_a$ and $\mathbf{H}_a$.

For this problem it will be assumed that both mirrors may be characterized by a single electric field reflection coefficient that presents an almost perfect short to the electric fields, i.e., $\Gamma \approx -1$. The representative mode equation may be written as

$$\frac{\partial^2 e_n(t)}{\partial t^2} + \left[\Omega_n^2 + \frac{\omega_n}{Q_n}\frac{\partial}{\partial t}\right]e_n(t) + \frac{1}{\langle\epsilon\rangle}\left[\frac{\omega_n}{Q_n} + \frac{\partial}{\partial t}\right]\int \sigma \mathbf{E}\cdot\mathbf{E}_n \, dv = -\frac{1}{\langle\epsilon\rangle}\left[\frac{\omega_n}{Q_n} + \frac{\partial}{\partial t}\right]\frac{\partial}{\partial t}\int \mathbf{P}\cdot\mathbf{E}_n \, dv \tag{8}$$

where ω_n is the optical frequency of the nth mode, Ω_n is the unloaded resonant frequency of the cavity for the nth mode, and Q_n is the unloaded Q of the nth mode. These parameters are defined as

$$\Omega_n = n\pi(L\sqrt{M_0\langle\epsilon\rangle})^{-1} \tag{9}$$

$$Q_n = \frac{n\pi}{4}\frac{(1 + |\Gamma|)^2}{1 - |\Gamma|^2}. \tag{10}$$

This equation corresponds to the mode equation used by Lamb. However, there are two important differences:

1) It has been assumed that the time-independent loss of the cavity results from imperfectly reflecting mirrors.

2) A time-varying loss has been included that is represented by the volume integral $\int \sigma\mathbf{E}\cdot\mathbf{E}_n \, dv$. The effect of including mirrors with a finite transmission coefficient is to create the three terms in (8) that include ω_n/Q_n as a multiplying factor.

[3] It will be assumed that the optical resonator has plane parallel mirrors and that diffraction effects may be neglected. Therefore, the fields in the cavity may be written as a sum of TEM waves.

B. Coupled-Mode Equations

This subsection concerns the coupled-mode equations that result from expanding the two volume integrals in (8) in terms of the normal modes. In order to do this, it will be necessary to make some assumptions about the time-dependence of the mode amplitudes and about the form of the polarization vector $\mathbf{P}$.

Since this analysis is restricted to time-invariant normal modes, the mode amplitude in (8) may be written as

$$e_n(t) = \mathcal{E}_n \exp j[\omega_n t + \varphi_n] + \text{complex conjugate} \tag{11}$$

where $\mathcal{E}_n$, ω_n, and φ_n are all time-independent.

The polarization vector may be written as

$$\mathbf{P} = \epsilon_0 \chi \mathbf{E} \tag{12}$$

where χ is complex and depends upon the discharge excitation, the optical power, and the axial position.

Performing the integration of the last volume integral in (8) merely evaluates the projection of the polarization vector onto the nth mode. This may be written as

$$\frac{1}{\epsilon}\int \mathbf{P}\cdot\mathbf{E}_n \, dv = \{\langle\chi_n\rangle - j\langle\text{loss tan}\rangle_n\}\mathcal{E}_n \cdot \exp j(\omega_n t + \varphi_n) \tag{13}$$

where $\langle\chi_n\rangle$ and $\langle\text{loss tan}\rangle_n$ are simply the average values of the real and imaginary parts of the susceptibility of the laser medium. The physical interpretation of these variables is that $\langle\chi_n\rangle$ is equal to the effective relative dielectric constant of the laser medium minus one and that $\langle\text{loss tan}\rangle_n$ is the average value of the loss (or gain) tangent of the laser medium. When the laser medium provides gain $\langle\text{loss tan}\rangle_n$ is less than zero. It will be convenient to express the magnitude of the gain tangent in terms of a dielectric Q as

$$Q_{ng}^{-1} = |\langle\text{gain tan}\rangle_n| \tag{14}$$

where the double subscript implies that it represents the gain of the medium for the nth mode.

It is convenient to express the frequency of the oscillating modes in terms of the resonant frequencies of the unloaded cavity $n\Omega_0$ as

$$\omega_n = n\Omega_0 - \delta_n. \tag{15}$$

In order to obtain a solution that may be expressed in terms of time-invariant mode amplitudes, the frequency separation between oscillating modes must be equal to the frequency of the time-varying loss. Thus, when the modes are coupled $\delta_{n+1} - \delta_n = \delta_0$ where δ_0 is a constant.

The next step in the analysis is to evaluate the coupling term represented by the projection of $\mathbf{E}$ onto the nth mode. This is evaluated in Appendix I. Substituting (34), (11), (13), (14), and (15) into (8) yields

$$\left\{\frac{2\delta_{0n}}{\omega_n} + jQ_n^{-1} + Q_\sigma^{-1}[j + Q_n^{-1}]\right\}\mathcal{E}_n - \frac{\cos(\pi Z_0/L)}{2Q_\sigma}[j + Q_n^{-1}] \times [\mathcal{E}_{n+1}\exp j(\varphi_{n+1} - \varphi_n + \omega_0 t_1) + \mathcal{E}_{n-1}\exp j(\varphi_{n-1} - \varphi_n - \omega_0 t_1)] = \{\langle\chi_n\rangle + Q_n^{-1}Q_{ng}^{-1} + j[Q_{ng}^{-1} - Q_n^{-1}\langle\chi_n\rangle]\}\mathcal{E}_n \quad (16)$$

where δ_{0n} is the value of δ_n when the modes are locked. It is apparent from the form of (16) that it has a trivial solution $\mathcal{E}_n = 0$. This results from the implicit approximation that neglected the spontaneous emission from the inverted population.

Recall that if the RF drive is reduced to zero, then $Q_\sigma = \infty$. Therefore, the mode equations for this condition may be obtained from (16) by simply letting Q_σ approach infinity. The real and imaginary parts of (16) may be equated separately to yield

$$\frac{2\delta_n}{\omega_n} = \langle\chi_n\rangle + Q_n^{-1}Q_{ng}^{-1} \quad (17)$$

and

$$1 = Q_nQ_{ng}^{-1} - \langle\chi_n\rangle \quad (18)$$

where δ_n is no longer a constant for all modes and the subscript zero must be dropped.

Using Lamb's assumption that the loss due to the mirrors is replaced by a volume conductivity, the resulting equations that would correspond to (17) and (18) would be

$$\frac{2\delta_n}{\omega_n} = \langle\chi_n\rangle \quad (17L)$$

and

$$1 = Q_nQ_{ng}^{-1}. \quad (18L)$$

The notation designating these as (17L) and (18L) is used to emphasize that Lamb's assumptions were used in their derivation.

It is clear that the results obtained by these different assumptions are equal only when the Q of the cavity is very high. When the Q is very high, the physical interpretations of (17) and (18) are: 1) the gain of the medium Q_{ng}^{-1} is equal to the loss of the cavity Q_n^{-1}. 2) the optical frequency of the nth mode differs from the unloaded resonant frequency of the cavity Ω_n by an amount that is proportional to $\langle\chi_n\rangle$. As the Q of the cavity is decreased, the frequency pulling by the medium will be affected by Q_{ng}^{-1}. Since the frequency pulling of the medium is small, i.e., $\langle\chi_n\rangle \ll 1$, the right-hand side of (18) is approximately $Q_n^{-1}Q_{ng}^{-1}$.

Harris and McDuff [10] analyzed a laser with an intracavity modulator [11] that varied the real part of the dielectric constant. This corresponds to the case treated by Gordon and Rigden [9]. The coupled-mode equation for this condition may be obtained from (16) by replacing Q_σ^{-1} by $j[\omega_n\Delta\epsilon/\langle\epsilon\rangle](\Delta Z/L)$, where $\Delta\epsilon$ is the magnitude of the change in the dielectric constant. Replacing Q_σ^{-1}, a real term, by an imaginary term changes the amplitude modulated output to a frequency modulated output under certain conditions.

C. Coupled-Mode Solutions

An approximate solution to the coupled-mode equation will be derived in this subsection. From this solution it will be possible to predict: 1) the pulse repetition frequency, 2) the pulse width, 3) the pulse amplitude, and 4) the effect of varying the frequency difference between the modulation frequency and the axial mode spacing on pulse position and average power. A simplifying assumption that will be used in the analysis is that all oscillating modes have the same amplitude and that all the other modes have zero amplitude. However, this restriction on mode amplitudes will be used only in the last stages of the analysis for maximum generality. Thus, the desired solution to the mode-coupled equation will provide the phase relationships between modes and the amplitude of a representative mode.

It will be necessary to make the following assumptions in order to proceed further:

1) It will be assumed that the frequency pulling by the medium on the center mode is unchanged by the time-varying loss, or equivalently, that $\delta_0' \propto \delta_0$ where $\delta_0' = \delta_{0n} - \delta_n$.
2) It will be assumed that all oscillating modes have the same amplitude and that the amplitude of the center mode is $\mathcal{E}_p$.
3) It will be assumed that the Q of the cavity is sufficiently high so that the imaginary part of the right-hand side of (16) is equal to $Q_{ng}^{-1}\mathcal{E}_n$. Furthermore,

$$Q_{ng}^{-1} = Q_{n0}^{-1} - \sum_m \beta_{nm}|\mathcal{E}_m|^2$$

where β_{nm} represents the saturating effect from the optical power in the mth mode on the gain of the nth mode and Q_{n0}^{-1} represents the small signal gain parameter. This β_{nm} corresponds to the saturating parameter derived by Lamb.

4) It will be assumed that the phase relationships between modes may be expressed as

$$\varphi_n = -n\omega_0 t_1 + \alpha_n \quad \text{for} \quad \cos(\pi Z_0/L) > 0$$

and

$$\varphi_n = -n(\omega_0 t_1 + \pi) + \alpha_n \quad \text{for} \quad \cos(\pi Z_0/L) < 0$$

where

$$\alpha_n \ll 1.$$

It is necessary to consider the conditions when $\cos(\pi Z_0/L) > 0$ and $\cos(\pi Z_0/L) < 0$ separately. Physically, the only difference between these two conditions is the choice of the origin for the z axis. The following analysis will be restricted to the condition that $\cos(\pi Z_0/L) > 0$. If the modulator were moved to the opposite end of the

laser, without changing the phase of the RF, the light pulse would be delayed by approximately one-half of the period between pulses.

Subtracting (17) from (16) yields

$$\left\{\frac{2\delta_0'}{\omega_n} + jQ_n^{-1} + Q_\sigma^{-1}[j + Q_n^{-1}]\right\}\mathcal{E}_n$$

$$- \frac{\cos(\pi Z_0/L)}{2Q_\sigma}[j + Q_n^{-1}][\mathcal{E}_{n+1} \exp j(\varphi_{n+1} - \varphi_n + \omega_0 t_1)$$

$$+ \mathcal{E}_{n-1} \exp j(\varphi_{n-1} - \varphi_n - \omega_0 t_1)] = jQ_{n_\sigma}^{-1}\mathcal{E}_n. \quad (19)$$

With the high Q approximation, the real part of (19) is satisfied if

$$\alpha_n = n^2\Phi/2p \quad (20)$$

where

$$\Phi = -4pQ_\sigma\delta_0'[\Omega_p \cos(\pi Z_0/L)]^{-1}. \quad (21)$$

Thus, the relative phase between modes may be written in terms of $\omega_0 t_1$ and Φ as

$$\varphi_{p+m} \approx \varphi_p + m(\Phi - \omega_0 t_1) \quad (22)$$

where the mode in the center of the oscillating line is denoted as the pth mode. The integer m had the maximum value of twenty during the experiments discussed in Section III.

The average power in the pth mode W_p as a function of RF drive may be obtained by substituting (22) into the imaginary part of (19). In the high Q approximation this yields

$$\frac{W_p(\infty) - W_p(Q_\sigma)}{W_p(\infty)} = \frac{1 - \cos(\pi Z_0/L)\cos\Phi}{Q_\sigma(Q_{p_\sigma}^{-1} - Q_p^{-1})} \quad (23)$$

where $\sum_m \beta_{pm}|\mathcal{E}_m|^2$ is replaced by βW_p since all modes are assumed to have the same amplitude.

Equation (23) represents the fractional reduction in optical power in a typical mode as the modulation drive is reduced from infinity, i.e., as the RF drive is increased from zero. The physical interpretation of (23) is that if the modulator is located at a mirror surface and the cavity length is adjusted so that $\Phi = 0$, i.e., the frequency of the time-varying loss is equal to a submultiple of the loaded-resonant cavity frequency as determined from (21), the average output power is unaffected by the RF drive. The term $(Q_{p_\sigma}^{-1} - Q_p^{-1})$ in the denominator of (23) represents the degree that the laser is operating above threshold. If the loss of the cavity as represented by Q_p^{-1} is just equal to the small signal gain, then $(Q_{p_\sigma}^{-1} - Q_p^{-1})$ is small and the reduction in output power is critically dependent upon cavity dimensions. However, if the laser is operating well above threshold, the term in the denominator is much larger and the fractional reduction in power is much smaller.

D. Effect of Mode-Locking

Locking the phase of each mode to its adjacent modes, as given by (22), causes the laser to operate as a pulse regenerative oscillator. This may be demonstrated by evaluating the total electric field at a mirror surface. When there are $2N + 1$ identical modes and $\mathcal{E}_p$ is the center mode, the total field E_t may be summed to yield

$$E_t = 2\mathcal{E}_p\left[\frac{\sin(N + \frac{1}{2})\gamma \cos(\gamma/2)}{\sin\gamma}\right] \exp j\omega_p t \quad (24)$$

where

$$\gamma = \omega_0(t - t_1) + \Phi. \quad (25)$$

Equation (24) is identical to the results obtained by DiDomenico [2] if $\Phi = 0$ and $Z_0 = 0$. The physical interpretation of (24) is that a light pulse occurs whenever $\gamma = 2n\pi$ where $n = 0, 1, 2, \cdots$. From (25), the phase of the light pulse relative to the RF is linearly dependent upon the difference in frequency of the time-varying loss and the fundamental cavity frequency. If $\Phi = 0$, the pulse occurs when the standing acoustic wave in the fused quartz is zero, independent of the position of the modulator in the optical cavity. The implication is that the light pulse is always at the mirror surface closest to the modulator when the modulator attenuation is zero. This explains why the average output power is optimized when the modulator is at a mirror surface. For all other positions the light pulse must pass through the modulator when it is slightly attenuating.

The ratio of peak power to average power and pulse width were also determined by DiDomenico, and it follows from (24) that

$$\frac{\text{Peak power}}{\text{Average power}} \approx \text{number of coupled modes}$$

$$\text{Pulse width } (\tfrac{1}{2}\text{ power}) \approx (\text{oscillating linewidth})^{-1}.$$

III. Experimental Results

The validity of the solutions to the mode-coupled equation presented in Section II may be evaluated from experimental results. The light pulses from a mode-locked laser were observed with a magnetically focused photo-multiplier tube (PMT) developed by Miller and Wittwer [12]. With a total accelerating voltage of 3.6 kV across the tube, the measured frequency response is flat from dc to greater than 3 kmc. A Hewlett-Packard sampling-oscilloscope with a rise-time of ~0.09 ns was used to observe the pulses from the PMT. The combined rise-time of the PMT and oscilloscope was ~0.14 ns.

The more important results that may be experimentally verified are listed:

1) The width of the pulse is approximately equal to the (oscillating linewidth)$^{-1}$ or $(\Delta\nu)^{-1}$.
2) The ratio of peak power to the average power is approximately equal to the number of coupled modes or $\Delta\nu/(c/2L)$.
3) The average output of the laser is a function of modulator drive and cavity tuning as given by (23).
4) The phase of the light pulse relative to the RF is linearly dependent upon the cavity tuning parameter Φ, as given by (21) and (25).

A. Pulse Width

Typical light pulses for the 6328 Å He–Ne and the 4880 Å Argon-Ion lasers are shown in Figs. 2 and 3. These pictures were obtained with a mirror spacing of 1.5 m and a pulse repetition rate of 100 Mc/s. The lower trace in Fig. 2 represents the 50-Mc/s RF voltage applied to the quantz transducer. This figure graphically displays the fact that the pulse repetition rate was twice the frequency of the applied RF. The absolute phase difference between the zero-crossings of the RF and the position of the light pulse was irrelevant since it was a function of the RF phase-shift in the tuned circuit that was used to provide an impedance match between the transmitter and the quartz transducer. However, it was possible to obtain the change in the phase difference between the train of light pulses and the RF when the cavity length was changed from oscilloscope displays similar to Fig. 2. Typical measured pulse widths from the He–Ne and the Argon-Ion lasers were 0.5 and 0.25 nanoseconds, respectively. These measurements were compatible with the expected oscillating linewidths of 2 kmc for the He–Ne laser and 4 kmc for the Argon-Ion laser. The fall-time for the Argon-Ion pulse was ~0.15 ns. The asymmetrical shape of the pulses and the ripple on the base lines shown in Figs. 2 and 3 were tentatively attributed to a second set of modes which were phase-locked but which had an axial mode spacing slightly different from the main set of modes. Unless reasonable care was used in tuning the cavity, this effect became so pronounced that a second train of light pulses was generated.

B. Peak Pulse Power

The measured ratio of the peak power to the average power for the He–Ne laser was 17, i.e., approximately equal to the number of oscillating modes. While the expected power ratio for the Argon-Ion laser was approximately 40, the measured value was between 20 to 30. This discrepancy was probably due to a nonuniform distribution of mode amplitudes.

C. Average Power

The measured change in average power resulting from small changes in cavity length is illustrated in Fig. 4(b). The nominal cavity length was 1.5 m. It is apparent that the cavity length designated as 3 mils of translation corresponded to the resonant condition, i.e., $\Phi = 0$ in (23), since the output power was a maximum for this position.

Equation (23) predicts that the average power is unaffected by RF drive at the resonant condition if $Z_0 = 0$. The measured reduction in power, when the cavity was adjusted to its resonant length and $Z_0/L = 0.04$, was typically much less than five per cent.

Note that when the length was decreased by 3 mils from this resonant condition, the average power was reduced to ten per cent of its maximum value. A further decrease in cavity length produced a condition that quenched the laser. Changing the cavity length by one mil changes its fundamental resonant frequency by less than two parts in 10^5. This demonstrates the fact that critical tuning was required.

The data plotted in Fig. 4(b) was obtained with a fixed RF drive. If this experiment is repeated several times with different values of RF drive, (23) predicts a family of curves which all peak at a particular cavity

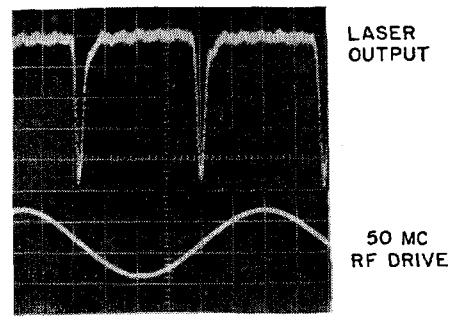

Fig. 2. Output signal from a mode-locked 6328 Å He–Ne laser.

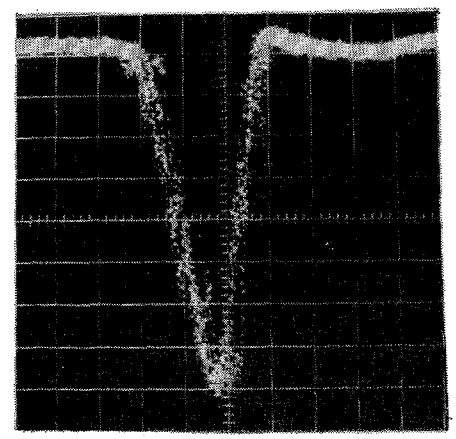

0.2 Nanosec/cm

Fig. 3. Output signal from a mode-locked 4880 Å Argon-Ion laser.

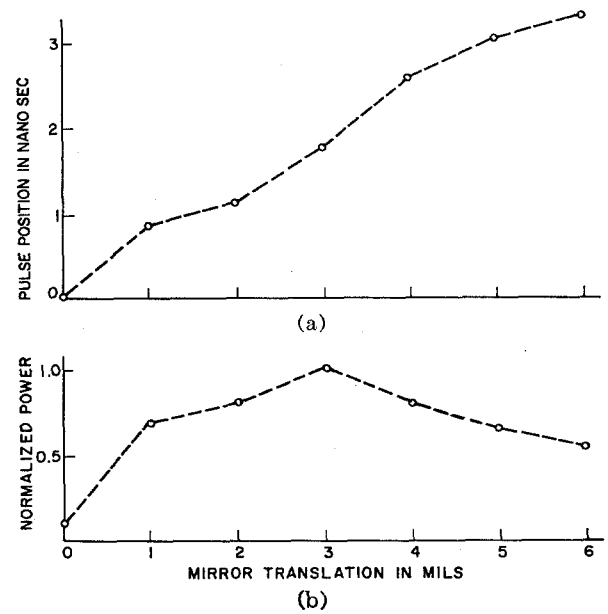

Fig. 4. Measured output power and pulse position vs. small changes in cavity length.

length. It was difficult to obtain consistent data in such an experiment since changing the RF drive changed the temperature of the fused quartz and, consequently, introduced a slow time-varying change in Q_σ. Thus, while the experimental results predicted by (23) have been essentially verified, more refined experiments are necessary to establish its absolute accuracy.

D. Pulse Position

The measured position of the light pulse relative to a constant frequency RF drive vs. a change in cavity length is plotted in Fig. 4(a). This data indicates the position of the light pulse, as measured from some arbitrary time, was essentially linearly dependent upon cavity length as predicted by (25). Changing the cavity length by one mil, i.e., $c/2L$ was changed by two parts in 10^5, pulled the light pulse by approximately one nano-second. This was approximately $\frac{1}{10}$ of the period between pulses when the cavity length was 1.5 m.

The preceding experimental results verify that the ad hoc assumptions used in deriving the effects of mode-coupling are reasonable and that the analysis based upon these assumptions provides some physical insight into characteristics of mode-coupled lasers.

IV. Self-Locking

In most cases, the important characteristics of a multimode laser may be predicted by assuming that the frequency and the phase of the optical modes are independent of each other. This section is concerned with a laser operating under the conditions for which these assumptions are not valid.

Experimental evidence of natural mode-coupling is described in the literature [5] in terms of the RF beats generated by a square-law detector. Reference is made to circumstances for which the amplitude and frequency stability of the beats are greatly increased. Figure 5 represents the output of a 6328 Å He–Ne laser as seen by a high-speed PMT without the use of an intracavity modulator. The display was obtained merely by optimizing the RF beats as observed on a spectrum analyzer. The period between pulses of 10 ns corresponds to a cavity length of 1.5 m. Comparing this figure with Figs. 2 and 3 reveals that this output resulted from coupled modes. This pulsating condition was obtained simply by reducing the Q of the cavity. The self-pulsing condition was obtained for cavity spacings ranging from 39 to 250 cm or repetition frequencies of 60 to 380 Mc/s. The Q of the cavity may be reduced to the appropriate value by inserting a time-independent loss into the cavity or by using high transmission mirrors. The photograph in Fig. 5 was obtained by using one high transmission mirror and one high reflecting mirror. While the Q was reduced under this condition, the laser was operated well above threshold.

A few attempts to operate the Argon-Ion laser in this condition have been uniformly unsuccessful.

The purpose of the next subsection is to provide some justification for the experimentally observed self-locked condition and the requirement that the Q be reduced.

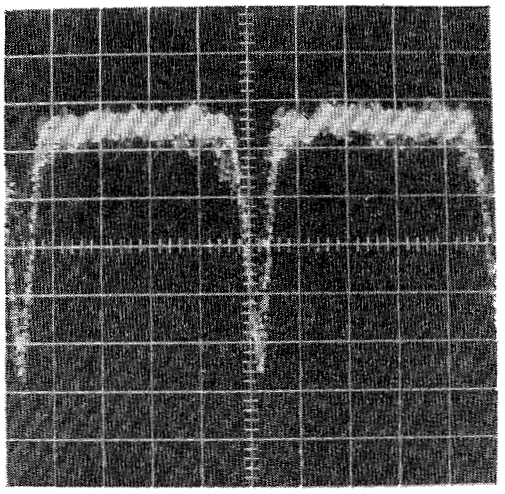

2×10^{-9} sec/cm

Fig. 5. Output signal from a 6328 Å He–Ne laser with naturally coupled modes.

A. Self-Locked Modes

Lamb [5] provides insight into the self-locked modes. Before discussing Lamb's analysis, it is instructive to examine the mode equations derived in a previous section that are valid when there are no time-varying losses in the cavity.

In Section III, $Q_{n\sigma}^{-1}$ was expanded in terms of the square of the mode amplitudes. A more accurate expansion, as indicated by Lamb, may be written as

$$Q_{n\sigma}^{-1} = Q_{n0}^{-1} - \sum_m \beta_{nm} |\mathcal{E}_m|^2 + \eta_n \mathcal{E}_{n+1}\mathcal{E}_{n-1} \cos(\varphi_{n+1} + \varphi_{n-1}) \quad (26)$$

where the last term represents a coupling term that is a function of the relative phase between adjacent modes.

Equations (17), (18), and (26) may be combined to yield

$$\frac{2\delta_n}{Q_n\omega_n} + Q_n^{-1} - Q_{n0}^{-1} + \sum_m \beta_{nm} |\mathcal{E}_m|^2 \approx \eta_n \mathcal{E}_{n+1}\mathcal{E}_{n-1} \cos(\varphi_{n+1} + \varphi_{n-1}). \quad (27)$$

It should be recalled that δ_n represents the frequency pulling by the medium and cannot be adjusted directly. However, it may be possible to adjust Q_n so that the left-hand side of (27) is a constant independent of n. If this is possible, (27) stipulates that the optical phases may be expressed as

$$\varphi_n = n\psi + \psi_0. \quad (28)$$

From Section III, it is known that this represents the phase relationship for a pulsating laser.

The preceding analysis has shown that the derived mode equations are compatible with the observed self-locked pulsating laser. Also, it demonstrates that judiciously adjusting the cavity Q is equivalent to varying the mode-coupling.

Lamb discusses the experimental condition required for a self-locked condition when there are only three oscillating modes. The result of this analysis, after certain approximations are made, is that locking will always occur when $\sin(\varphi_{n+1} + \varphi_{n-1} - 2\varphi_n)$ equals zero, if the small gain parameter Q_{n0}^{-1} for the center mode is equal to $\frac{1}{2}$ the sum of the small gain parameters for the adjacent modes. This condition is also satisfied when the small gain parameter is the same for all modes. This is precisely the condition required to make the laser operate as a pulse regenerative oscillator and is equivalent to (28), which was obtained from (27).

The previous statements and conclusions are valid only when adjacent mode-coupling effects are present, and they are much greater than the effects of mode coupling from more distant modes. Thus, if a laser is operated with mode separations that are very large or very small, it may be impossible to operate it as a self-locked laser.

Since the natural linewidth of the Argon-Ion laser is about ten times the linewidth of the He–Ne laser, the proper cavity length to produce a self-locked Argon-Ion laser should be much less than the proper length for the He–Ne laser. Experiments are being considered that will evaluate the accuracy of this hypothesis.

V. Conclusions

The effect of coupling the modes in a laser by inserting a time-varying loss into the cavity or by the nonlinear gain characteristics of the inverted population is evaluated. The dominant characteristic resulting from this coupling is that the laser operates as a pulse regenerative oscillator which produces narrow pulses of light. The width of these pulses is approximately equal to (oscillating linewidth)$^{-1}$. When the modes are coupled with a time-varying loss the pulse repetition rate will be equal to the frequency of the time-varying loss. When the modes are coupled naturally by the medium, the pulse repetition rate is approximately equal to the frequency of the axial mode spacing.

The conditions that are necessary to lock the modes together naturally are also discussed. It has been demonstrated that a 6328 Å He–Ne laser may be self-locked by judiciously adjusting the Q of the cavity.

In designing a communication system which uses a multimode laser, it is necessary to consider the characteristics of the self-locked condition. For example, if a multimode laser is used as a CW-light source in a communication system and the modes occasionally become self-locked, the distortion resulting from the light pulses, which may be twenty times the average light level, will render the system useless in most circumstances. Hence, it is necessary to insure that the laser is always in the mode-locked condition or that it will never be in the self-locked condition. One practical solution is to insert a time-varying loss into the cavity to insure that the modes are always locked.

The subnanosecond pulses from a mode-locked laser have proven to be very useful in determining the response of high-speed photodetectors.

Appendix I

The purpose of this Appendix is to evaluate the coupling between modes as given by the third term in (8). This term may be wrtiten as

$$\frac{1}{\langle\epsilon\rangle}\left[\frac{\omega_n}{Q_n}+\frac{\partial}{\partial t}\right]\int_{Z_0-\Delta Z/2}^{Z_0+\Delta Z/2}\sigma(Z,t)\cdot\sum_b\frac{2}{L}[e_b(t)\sin k_bZ\sin k_nZ]\,dZ \tag{29}$$

where $\sigma(Z, t)$ is given by (1). This equation may be rewritten as

$$\text{C.T.} = \frac{\sigma_1}{L\langle\epsilon\rangle}\left[\frac{\omega_n}{Q_n}+\frac{\partial}{\partial t}\right]\left[1-\cos\omega_0(t-t_1)\right]\cdot\sum_b\int_{Z_0-\Delta Z/2}^{Z_0+\Delta Z/2}[\cos(k_b-k_n)Z-\cos(k_b+k_n)Z]\,dZ \tag{30}$$

where C.T. represents the coupling term. Since $\cos(k_b + k_n)Z$ varies very rapidly with Z, (30) may be written as

$$\text{C.T.} = \frac{\sigma_1}{\langle\epsilon\rangle}\left[\frac{\omega_n}{Q_n}+\frac{\partial}{\partial t}\right]\cdot[1-\cos\omega_0(t-t_1)]\sum_b e_b(t)A_{bn} \tag{31}$$

where

$$A_{bn} = \frac{\sin k_{bn}\Delta Z/2\,\cos k_{bn}Z_0}{k_{bn}L/2} \tag{32}$$

$$A_{nn} \approx \Delta Z/L \tag{33}$$

and

$$k_{bn} \equiv k_b - k_n.$$

Since $\omega_0 \approx \omega_{n+1} - \omega_n$ and this analysis is restricted to adjacent mode coupling, (31) may be approximated as

$$\begin{aligned}\text{C.T.} = {}& \frac{\omega_n^2}{Q_nQ_\sigma}\left\{e_n(t)-\frac{\cos(\pi Z_0/L)}{2}\cdot[[\mathcal{E}_{n+1}\exp j[(\omega_{n+1}-\omega_0)t+\varphi_{n+1}+\omega_0t_1]\right.\\ &\left.+\mathcal{E}_{n-1}\exp j[(\omega_{n-1}+\omega_0)t+\varphi_{n-1}-\omega_0t_1]]]\right\}\\ &+j\frac{\omega_n}{Q_\sigma}\left\{\omega_ne_n(t)-\frac{\cos(\pi Z_0/2)}{2}\cdot[[(\omega_{n+1}-\omega_0)\mathcal{E}_{n+1}\exp j[(\omega_{n+1}-\omega_0)t+\varphi_{n+1}+\omega_0t_1]\right.\\ &\left.+(\omega_{n-1}+\omega_0)\mathcal{E}_{n-1}\exp j[(\omega_{n-1}+\omega_0)t+\varphi_{n-1}-\omega_0t_1]]]\right\}.\end{aligned} \tag{34}$$

When (34) is substituted into (8), it is apparent that if $\mathcal{E}_n(t)$ is independent of time, $\omega_{n+1} - \omega_0 = \omega_{n-1} + \omega_0 = \omega_n$. Equation (34) is simplified with this assumption.

VI. Acknowledgment

The author wishes to express gratitude to E. I. Gordon for many fruitful discussions.

References

[1] Cutler, C. C., The regenerative pulse generator, *Proc. IRE*, vol 43, Feb 1955, pp 140–148.
[2] DiDomenico, M., Jr., Small-signal analysis of internal (coupling-type) modulation of lasers, *J. Appl. Phys.*, vol 33, Oct 1964, pp 2870–2876.
[3] Yariv, A., Internal modulation in multimode laser oscillators, *J. Appl. Phys.*, vol 36, Feb 1965, pp 388–391.
[4] Hargrove, L. E., R. L. Fork, and M. A. Pollack, Locking of He-Ne laser modes induced by synchronous intracavity modulation, *J. Appl. Phys. (Lett.)*, vol 5, Jul 1964, pp 4–5.
[5] Lamb, W. E., Jr., Theory of an optical maser, *Phys. Rev.*, vol 134, Jun 1964, pp A1429–A1450.
[6] Cook, B. D., and E. A. Aiedemann, Diffraction of light by ultrasonic waves of various standing wave ratios, *J. Acoust. Soc. Amer.*, vol 33, 1961, pp 945–948.
[7] Damaria, A. J., Ultrasonic control of laser action, *Symp. on optical masers of Poly. Tech. Inst. of Brooklyn*, Apr 1963, pp 253–269.
[8] Slater, J. C., *Microwave Electronics*. Princeton, N. J.: Van Nostrand, 1959, pp 253–269.
[9] Gordon, E. I., and J. D. Rigden, The Fabry-Perot electrooptic modulator, *Bell Sys. Tech. J.*, vol 42, Jan 1963, pp 155–179.
[10] Harris, S. E., and O. P. McDuff, *J. Appl. Phys. (Lett.)*, vol 5, Nov 1964, pp 205–206.
[11] Harris, S. E., and R. Targ, *J. Appl. Phys. (Lett.)*, vol 5, Nov 1964, pp 202–204. Under certain conditions this form of intracavity modulation produces a distribution of mode amplitudes that resembles the Bessel function distribution of a pure FM signal.
[12] Miller, R. C., and N. C. Wittwer, Secondary emission amplification at microwave frequencies, *IEEE J. of Quantum Electronics*, vol QE-1, Apr 1965, pp 12–20.

Performance of Laser-Pumped Quantum Counters

WILLIAM F. KRUPKE

Abstract—Narrow-band quantum counters with less than unit internal quantum efficiency are analyzed. The pump power dependent expressions for the transient and steady-state quantum efficiencies are derived. These quanties are discussed for "typical" trivalent and divalent rare-earth-doped insulator crystals, and the performance of two specific systems is presented. It is shown that to achieve high quantum efficiency in trivalent rare-earth-doped quantum counter systems, the pump source must be highly nonblackbody in spectral character, i.e., a laser, and resonant with the transition between the relevant excited states. Performance limiting factors for laser-pumped quantum counters are pointed out.

Introduction

THE NARROW-BAND quantum counter (QC) was first proposed by Bloembergen [1], [2] in 1958. The mechanism essential to quantum counter action is the near-simultaneous absorption of a resonant infrared or ultramicrowave [3] signal quantum and a "local" pump quantum. This event is followed by emission of a single quantum of higher energy, which is detected by a conventional broadband detector. A net improvement in detectivity of the signal quantum can result when conventional detectors sensitive to the signal radiation wavelength have poor signal-to-noise ratios, (SNR) while those sensitive to the output emission wavelength have good SNR. In 1959, Gelinas [4] made a detailed comparison of the performance and detectivity of an *ideal* infrared QC and *ideal* infrared broadband detectors in the presence of various signal and background spectral distributions. (An ideal detector is one with no internal noise and unit quantum efficiency for radiation falling within its spectral region of sensitivity.) The principal conclusion of this study is that an *ideal* QC can exhibit superior detectivity compared to an *ideal* broadband detector *only* when detecting nearly monochromatic signal radiation with a wavelength matching that of the QC. Neither methods of generating appreciable amounts of monochromatic signal radiation just matching the sensitive wavelength of the QC nor methods of building a QC approaching the ideal were considered.

An experimental QC to detect 2.3μ quanta by utilizing the atomic energy levels of Pr^{3+} ions embedded in a $LaCl_3$ crystalline host lattice was proposed by Porter [5] in May 1961 and operated by Porter [6] in Dec. 1961. The two-photon absorption process was demonstrated in this experiment, but it did not result in a practical device for reasons given later in this report. Brown and Shand produced similar results at wavelengths of 1.4, 1.5, 1.9, and 4.2μ in other praseodymium-doped host lattices, [7] and at wavelengths of 0.65, 1.13, and 1.5μ in fluoride host lattices doped with trivalent erbium [8]. A variant form of QC action, incoherent frequency down-conversion, was experimentally observed by Halsted, et al. [9], [10] in sulphide phosphors by using the lattice band states and the broad impurity levels of copper. In one case, a single signal quantum at a wavelength of 3480 Å produced 160 fluorescent quanta at a wavelength of 1.56μ.

At this point in the technological development of quantum counters, it seems useful to inquire into the practicability of constructing a QC device approaching the ideal. In this paper, rare-earth (RE)-doped materials are considered as a class of substances suitable for this purpose. Recent technological advances in related fields which may be of use in this quest are also discussed.

Theoretical Improvement in Minimum Detectable Power

The energy level scheme of the quantum-counter system studied in detail is shown in Fig. 1. The signal transition takes place between levels 1 and 2 at an angular fre-

Manuscript received January 21, 1965. This work was supported by United States Air Force under Contract No. AF 04(695)-269.
The author is with Quantum Electronics Dept., Aerospace Corp., El Sequndo, Calif.